

## Thermal behavior of LDH $2\text{CuAl}(\text{CO}_3)$ and $2\text{CuAl}(\text{CO}_3)/\text{Pd}$

V. A. Neves<sup>1</sup> · M. V. Costa<sup>1</sup> · J. D. Senra<sup>2</sup> · L. C. S. Aguiar<sup>1</sup> · L. F. B. Malta<sup>1</sup> 

Received: 21 December 2016 / Accepted: 19 April 2017 / Published online: 27 April 2017  
© Akadémiai Kiadó, Budapest, Hungary 2017

**Abstract** Cu/Al layered double hydroxide (LDH) can be used as a catalyst for important processes such as cross-coupling reactions. This property may be improved by adding palladium by either impregnation or intercalation. Therefore, the LDH matrix and its composites with  $\text{Pd}^0$  or  $[\text{PdCl}_4]^{2-}$  have been prepared. By powder X-ray diffraction, FT-infrared spectroscopy, thermogravimetric and elemental analysis it was determined the LDH formula  $\text{Cu}_4\text{Al}_2(\text{OH})_{12}\text{CO}_3 \cdot 4\text{H}_2\text{O}$ , with malachite as the second phase. The LDH thermal decomposition occurs between 120 and 600 °C, having as intermediates the double oxihydroxide and the mixed oxide phases. At 800 °C the residue is composed of CuO and  $\text{CuAl}_2\text{O}_4$ . The composites were obtained employing  $[\text{PdCl}_4]^{2-}$  and  $\text{Pd}_2(\text{dba})_3$  as precursors, and the solvent choice for this process was shown to be of significant importance: the materials obtained using DMF had Pd impregnated in the surface, while the usage of water promoted the intercalation of  $[\text{PdCl}_4]^{2-}$  in the LDH matrix. The thermogravimetric analysis was able to distinguish the mode of supporting palladium between the composites being a reliable characterization for such task.

**Keywords** Layered double hydroxide · Copper · Palladium · Impregnation · Intercalation

### Introduction

Layered double hydroxides (LDHs), also known as anionic clays or hydrotalcite-like compounds, are natural or synthetic solid compounds composed by layers of metallic hydroxides and interlayer spaces filled with anions and neutral molecules. Its structure is based on brucite's ( $\text{Mg}(\text{OH})_2$ ), with partial substitution of bivalent cations by trivalent ones that introduces positive charges in the layers, and for the structure to be held together there is a need to be balanced with interlayer anions [1–5].

The LDHs can be described by the formula:  $M_{1-x}^{\text{II}}M_x^{\text{III}}(\text{OH})_2A_{x/n}^{n-} \cdot \delta\text{H}_2\text{O}$ , where  $M^{\text{II}}$  and  $M^{\text{III}}$  are, respectively, the bi- and trivalent cations and  $A^{n-}$  is the  $n$ -charged interlayer anion. They can be represented by alternative nomenclature, such as Mills' (International Mineralogical Association): LDH  $xM^{\text{II}}_yM^{\text{III}}.A[\text{B}]-Pt$ , where  $x$  and  $y$  are the metals proportion in the formula, B is a complex anion and  $Pt$  is the crystal polytype of the compound [3].

Usually the ratio  $M^{\text{II}}/M^{\text{III}}$  is 2:1 or 3:1, always with the majority of  $M^{\text{II}}$ . The anion influences the stability of the material, being the  $\text{CO}_3^{2-}$  the most stabilizing and common anion found in these compounds [4, 5].

These materials have received much attention in the last decades, because of its technological applications such as ion exchangers, flame retardancy agents, catalysts and support for metallic nanoparticles [1, 6–9], whereas they have been used with palladium as catalysts for cross-coupling reactions, as the Suzuki reaction [10–12].

**Electronic supplementary material** The online version of this article (doi:10.1007/s10973-017-6411-4) contains supplementary material, which is available to authorized users.

✉ L. F. B. Malta  
lfbmalta@iq.ufrj.br

<sup>1</sup> Instituto de Química, Universidade Federal do Rio de Janeiro, Cidade Universitária, Rio de Janeiro 21941-909, Brazil

<sup>2</sup> Instituto de Química, Universidade do Estado do Rio de Janeiro, Maracanã, Rio de Janeiro 20550-900, Brazil

C–C and C–N cross-coupling reactions are imperative in the synthesis of many organic structures with biological and electro-optics applications [13–16]. Considering the formation of C–N bonds [17] a composite material composed of Cu/Al LDH and Pd could be active for the N-arylation reaction since both catalytic approaches would be considered, the Ullmann–Goldberg [15] and the Buchwald–Hartwig [16] type reactions. However, one must be aware about the integrity of the layered catalyst at usual temperatures of 100 °C or beyond that are applied in catalytic processes having high-boiling point solvents. This is the temperature range to which the Cu/Al LDH has never had its stability tested. The proposal of the present work is to screen by thermal analysis the LDH stability and, concerning the composites, to infer the mode the LDH supports palladium and how to tune this.

## Experimental

### Synthesis of the LDH

The LDH was synthesized by coprecipitation at constant pH = 8 simultaneously mixing an aqueous solution 0.225 M  $\text{Cu}(\text{NO}_3)_2 \cdot 3\text{H}_2\text{O}$  and 0.075 M  $\text{Al}(\text{NO}_3)_3 \cdot 9\text{H}_2\text{O}$ —ratio Cu/Al = 3:1 with an alkali solution 0.50 M NaOH and 0.15 M  $\text{Na}_2\text{CO}_3$  into a solution  $10^{-6}$  M NaOH (pH = 8). The coprecipitation was carried out under magnetic stirring at ambient temperature and the pH remained 8 during the process. A blue gel was precipitated, and it was isolated by centrifugation. The calcinations at different temperatures (120, 200, 400, 600 and 800 °C) were done in furnace for 1 h using alumina crucible.

### Synthesis of the composites LDH/Pd

The composites of LDH with Pd were obtained by mixing the LDH during 24 h at 80 °C under magnetic stirring with 0.025 M  $\text{Na}_2\text{PdCl}_4$  or 0.012 M  $\text{Pd}_2(\text{dba})_3$  solutions in *N,N*-dimethylformamide (DMF), affording LDH/Pd1 and LDH/Pd2 materials, and with 0.025 M  $\text{Na}_2\text{PdCl}_4$  solution in water, obtaining the LDH/Pd3 material. After each process, the solid was isolated by vacuum filtration and dried at room temperature.

### Methods

The powder X-ray diffraction (XRD) patterns were obtained with a Rigaku diffractometer Ultima IV, 2 kW, using  $\text{CuK}\alpha$  with  $\text{k}\beta$  Ni filter and step of  $0.05^\circ$  in the range of  $5^\circ$ – $80^\circ$ . The FT-infrared spectra (FTIR) were obtained with a Nicolet Magna-IR spectrometer with  $4\text{ cm}^{-1}$  resolution in the range of  $400$ – $4000\text{ cm}^{-1}$ , and the samples

were mixed with KBr in order to have 1% pellets. The element quantification by energy-dispersive X-ray spectroscopy (EDS) was performed in a JEOL JSM 6460-LV microscope. The CHN elemental analysis was carried out using a ThermoFinnigan elemental analyzer FlashEA 1112. The thermogravimetric (TG) curves were acquired in SHIMADZU DTG-60 analyzer, applying  $5\text{ }^\circ\text{C min}^{-1}$  in argon or synthetic air, under a  $50\text{ mL min}^{-1}$  flow rate.

## Results and discussion

The XRD pattern of the Cu/Al LDH is shown in Fig. 1a, and it evidences the characteristic hydroxalcalite-like structure peaks in  $2\theta = 11.6^\circ$  (003),  $23.5^\circ$  (006),  $35.5^\circ$  (012),  $40.2^\circ$  (015),  $47.8^\circ$  (018) and  $63.0^\circ$  (110), indexed in accordance with the literature [1]. It was identified a second phase of  $\text{Cu}_2(\text{OH})_2\text{CO}_3$ , malachite, identified by *Crystmet* #561579 card.

Using the *Bragg Law* it was possible to calculate the interlayer distance of the LDH:  $d_{(003)} = 0.759\text{ nm}$ . The lattice parameters *c* and *a* were also determined:  $c = 3 \times d_{(003)} = 2.275\text{ nm}$  and  $a = 2 \times d_{(110)} = 0.295\text{ nm}$ ; these values had good agreement with previously data in the literature [2].

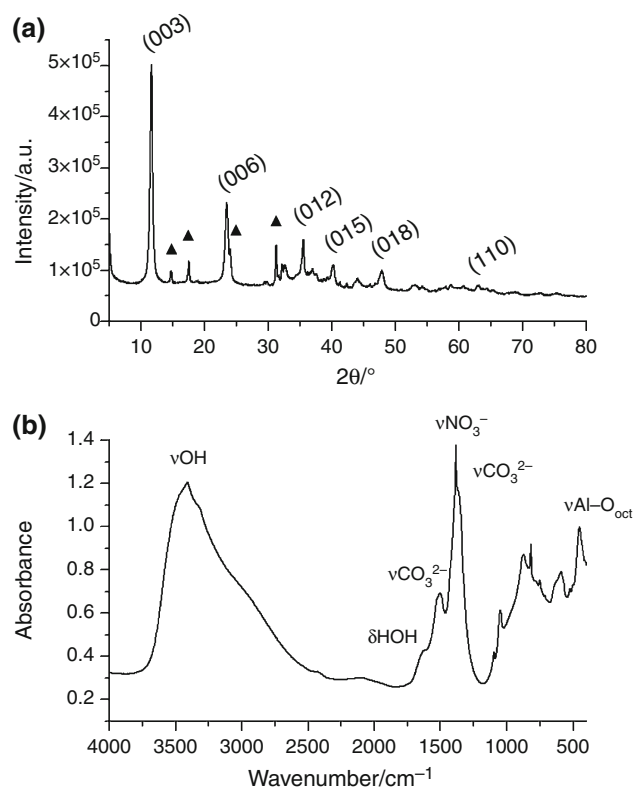


**Fig. 1** a Powder XRD pattern and b FTIR spectrum of LDH  $2\text{CuAl.CO}_3$ . Legend: (filled triangle)  $\text{Cu}_2(\text{OH})_2\text{CO}_3$

The crystallite size was calculated using the *Scherrer formula* for the peaks (003), (006) and (012):

$$T = \frac{0.9\lambda}{\beta \cos\theta} \quad (1)$$

in which  $T$  is the mean crystallite size,  $\lambda$  is the wavelength,  $\theta$  is the scattering angle and  $\beta$  is the maximum width at half-height. Its calculated value was 25 nm.

In the FTIR spectrum, as shown in Fig. 1b, the following vibration modes can be assigned:  $\nu$ O-H at 3410  $\text{cm}^{-1}$ , related to the LDH's hydroxyls and superficial water;  $\delta$ H-O-H at 1631  $\text{cm}^{-1}$ , from interlayered and hydrated water; asymmetric  $\nu$ C-O at 1355 and 1504  $\text{cm}^{-1}$ , from interlayer carbonate; asymmetric  $\nu$ N-O at 1384  $\text{cm}^{-1}$  from interlayer nitrate; and  $\nu$ Al-O at 451  $\text{cm}^{-1}$  related to the Al-O bond in octahedral geometry [6].

The elemental analysis by CHN and EDS (Tables 3 and 4, supplementary material) permitted the obtainment of  $\text{CO}_3^{2-}$  (0.21 mol/100 g),  $\text{NO}_3^-$  (0.01 mol/100 g, neglected due to the low quantity), Cu (0.72 mol/100 g) and Al (0.28 mol/100 g) quantities in the material. With these values it was possible to determine the LDH formula as  $\text{Cu}_4\text{Al}_2(\text{OH})_{12}\text{CO}_3$ , and the proportion between LDH and malachite in the sample was 94:6%. The actual Cu/Al ratio in the LDH was 2:1, different from the nominal ratio of 3:1. According to Mill's nomenclature [3] the LDH was denominated LDH 2CuAl<sub>2</sub>CO<sub>3</sub>.

With the TG analysis under synthetic air (Fig. 2) it was identified four temperature segments for the thermal decomposition of the layered compound, shown in Table 1 with its respective mass loss values. The LDH was calcined in each specific temperature. The XRD patterns and FTIR spectra are shown in Fig. 3.

At 120 °C (Fig. 3a) it was observed the beginning of the thermal decomposition process of the LDH, with the

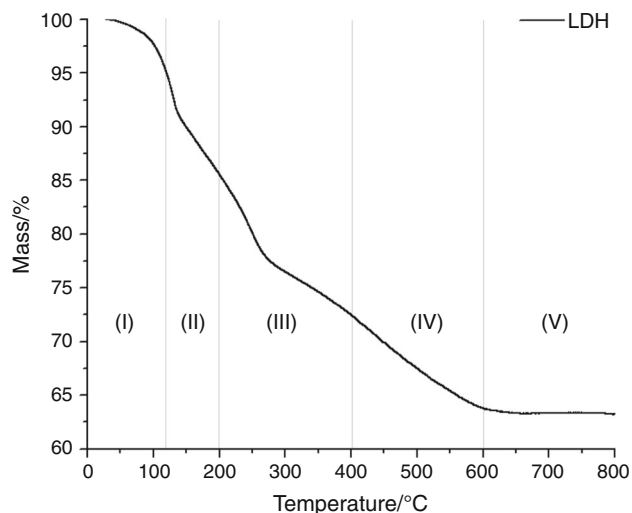
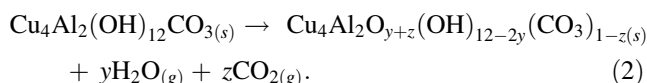


Fig. 2 TG curves data from the LDH 2CuAl<sub>2</sub>CO<sub>3</sub>

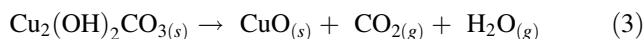
**Table 1** Mass loss values of the LDH 2CuAl<sub>2</sub>CO<sub>3</sub> (synthetic air)

| Temperature/°C | LDH 2CuAl <sub>2</sub> CO <sub>3</sub> |                | Malachite (calculated)/% |
|----------------|----------------------------------------|----------------|--------------------------|
|                | (Observed)/%                           | (Calculated)/% |                          |
| 25–120         | 6.7                                    | –              | –                        |
| 120–200        | 10.7                                   | 25.0           | –                        |
| 200–400        | 12.2                                   | –              | 1.7                      |
| 400–600        | 4.4                                    | –              | –                        |
| 600–800        | 0.9                                    | –              | –                        |

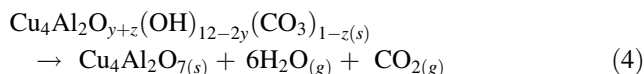
displacement of the peak (003) from 11.6° ( $d_{(003)} = 0.759$  nm) to 13.1° ( $d_{(003)} = 0.676$  nm) (stage I). This could be assigned to the interlayer water loss as shown by the weakening of the  $\delta$ HOH mode in the FTIR spectrum (Fig. 3b, r.t. and 120 °C spectra). At 200 °C this XRD peak was displaced to 13.9° (0.637 nm) and the baseline became curved, evidencing the presence of an amorphous phase, probably the double oxi-hydroxide derived from the LDH decomposition. The process related to this stage (II) can be represented by the following chemical reaction:



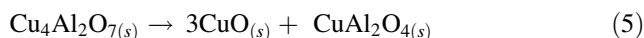
Between 200 and 400 °C (stage III) the malachite was decomposed and CuO was formed:



In addition the decomposition of the LDH ends at 600 °C when no significant carbonate bands are seen in the IR spectrum (stage IV):



And at 800 °C it was identified the growth of the final phases of CuO and CuAl<sub>2</sub>O<sub>4</sub> phase (stage V):



Concerning the water content,  $x$ , the process  $\text{Cu}_4\text{Al}_2(\text{OH})_{12}\text{CO}_3 \cdot x\text{H}_2\text{O} \rightarrow \text{Cu}_4\text{Al}_2\text{O}_7$  allowed the calculation of  $x = 4$ . Most of the hydrated water loss occurs in the stages I and II.

With the proposed reactions for the stages II, III and IV of the LDH thermal decomposition, it was observed an excellent agreement between the theoretical and the experimental mass losses (25.0 and 25.6%, respectively; Table 1).

Regarding the LDH/Pd composites, the diffraction patterns of LDH/Pd1 and LDH/Pd2 (Fig. 5) show that the LDH matrix was maintained and the (003) peak was kept in the same position, meaning no intercalation process; for the latter sample this was expected since it corresponded to the use of a Pd<sup>0</sup> containing precursor that either way would not

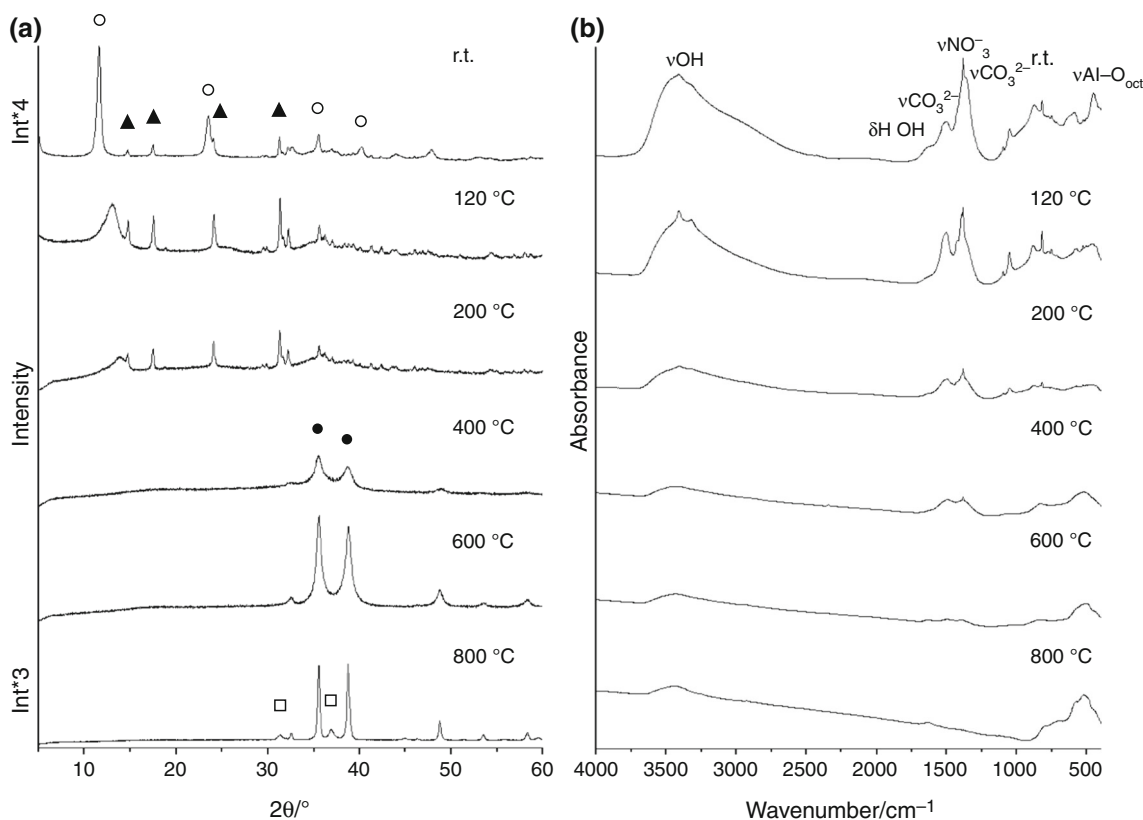


**Fig. 3** **a** Powder XRD pattern and **b** FTIR spectra of LDH  $2\text{CuAl}.\text{CO}_3$  calcined at different temperatures. Legend: (*open circle*) LDH  $2\text{CuAl}.\text{CO}_3$ , (*filled triangle*)  $\text{Cu}_2(\text{OH})_2\text{CO}_3$ , (*filled circle*)  $\text{CuO}$ , (*open square*)  $\text{CuAl}_2\text{O}_4$

be intercalated by ion exchange. For both it was observed the presence of  $\text{Pd}^0$  (111) peak at  $39.4^\circ$  meaning that a Pd reduction step took place for LDH/Pd1. The corresponding FTIR spectra exhibit the same band profile of the LDH matrix, including the presence of carbonate and Al–O bands. This corroborates the results from XRD that there was only a surface impregnation.

Their thermal decomposition profile shows differences in relation to the LDH profile mainly in the stages IV (both) and V (LDH/Pd1): stage IV is related to the final process of dehydration and decarbonation, and in stage V there is an extra mass loss of 3.5% in the 600–800 °C interval related to the formation of molecular chlorine from chloride ions associated with Pd.



Therefore, it leads to the conclusion that still some Pd remained unreduced in the LDH/Pd1 sample which makes it differ from the LDH/Pd2 sample. The Pd reduction process during ion exchange in DMF has already been reported by our group in a previous work for Mg/Al LDH [9].

The diffraction pattern of LDH/Pd3 (Fig. 4a) shows a new phase in the material, which could be interpreted as

the exchanged form of LDH with formula  $\text{Cu}_4\text{Al}_2(\text{OH})_{12}[\text{PdCl}_4]$ , with interlayer space of  $d_{(003)} = 0.546$  nm; no  $\text{Pd}^0$  peak was observed. A decrease in the interlayer distance was also reported in the intercalation process of  $[\text{PdCl}_4]^{2-}$  in Mg/Al LDH by Zhang et al. [12]; however, the reported shift of the (003) peak was not of such high magnitude (from  $d_{(003)} = 0.759$  nm in the LDH  $2\text{CuAl}.\text{CO}_3$  to 0.546 nm). In Fig. 4a it was noticed that the high intensity (003) peak dislocated from its original position at  $2\theta = 11.70^\circ$  for LDH to  $11.40^\circ$  for LDH/Pd3. This could really be showing the intercalation of  $[\text{PdCl}_4]^{2-}$ : in this case the peak with  $d = 0.546$  nm would be relative to an unknown new phase, most probably containing Pd. We are researching the identity of this phase to verify this hypothesis. The FTIR spectrum shows that the bands related to carbonate vibration modes have lost much of their intensity, reaffirming the chemical modification of the interlayer space. Its thermogravimetric curve (Fig. 5, green curve) shows significant difference from those of the others LDH signaling that the processes related to the mass losses tend to occur at higher temperatures. This is shown in Table 2: while for the others LDHs significant mass losses occur from 120 °C ahead, for LDH/Pd3 this

**Fig. 4** **a** Powder XRD pattern and **b** FTIR spectra of LDH 2CuAl<sub>2</sub>CO<sub>3</sub> and its composites with Pd. Legend: (open circle) LDH 2CuAl<sub>2</sub>CO<sub>3</sub>, (filled diamond) Pd<sup>0</sup>, (filled circle) Unknown new phase

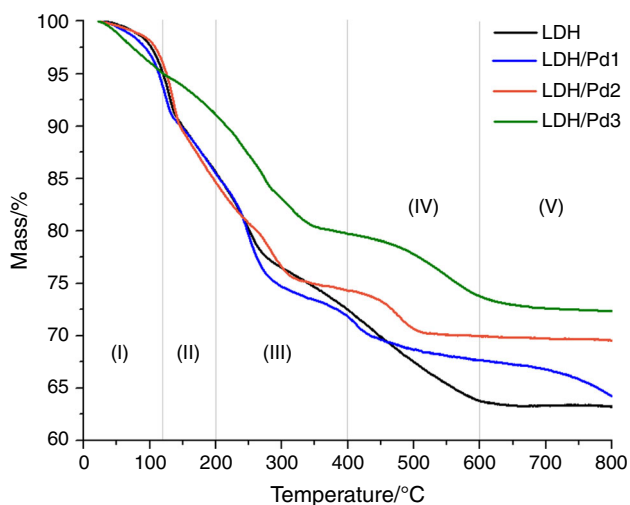
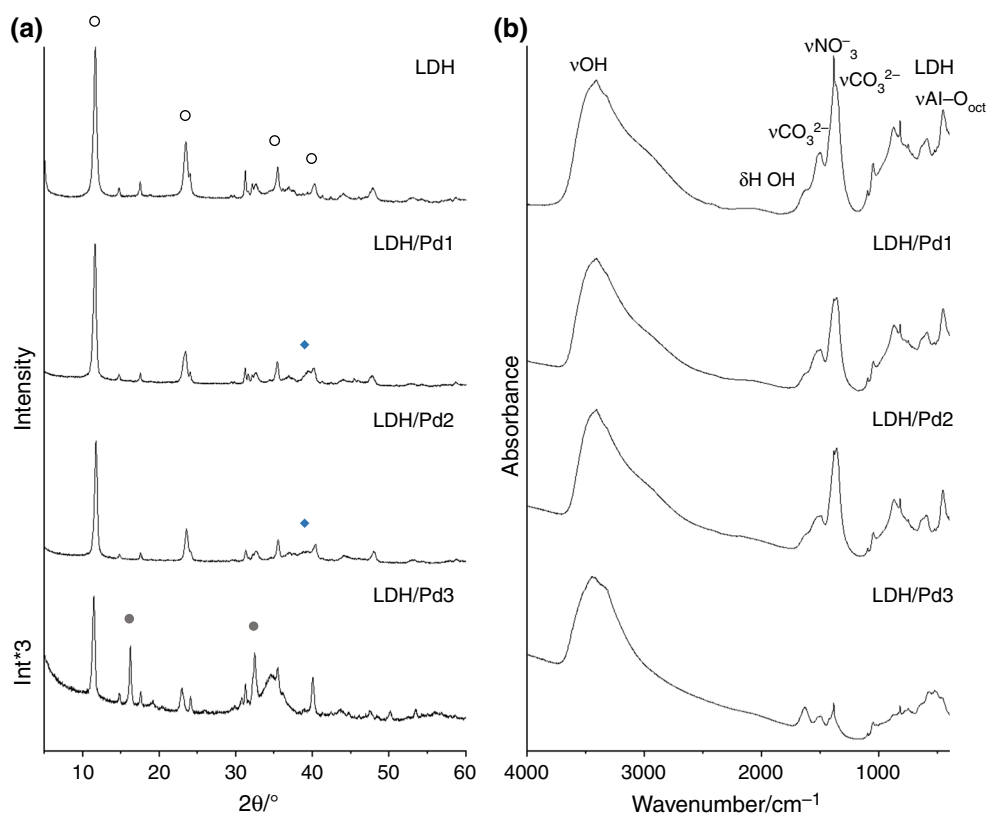


**Fig. 5** TG curves data from the LDH 2CuAl<sub>2</sub>CO<sub>3</sub> and its composites with Pd

only happens above 200 °C. The fact that this sample is maintained stable for higher temperatures could probably be related to the intercalation of a non-volatile ion [PdCl<sub>4</sub>]<sup>2-</sup>.

These results are consistent with the ion exchange process in the interlayer space between CO<sub>3</sub><sup>2-</sup> and [PdCl<sub>4</sub>]<sup>2-</sup>.

**Table 2** Mass loss % for the LDH 2CuAl<sub>2</sub>CO<sub>3</sub> and its composites with Pd (argon atmosphere)

| Temperature/<br>°C | LDH/<br>% | LDH/Pd1/<br>% | LDH/Pd2/<br>% | LDH/Pd3/<br>% |
|--------------------|-----------|---------------|---------------|---------------|
| 25–120             | 5.0       | 6.3           | 4.0           | 5.0           |
| 120–200            | 9.5       | 8.3           | 11.4          | 3.9           |
| 200–400            | 13.1      | 13.6          | 10.3          | 11.4          |
| 400–600            | 8.7       | 4.2           | 4.4           | 5.9           |
| 600–800            | 0.9       | 3.5           | 0.4           | 1.4           |

## Conclusions

The LDH Cu/Al with the formula Cu<sub>4</sub>Al<sub>2</sub>(OH)<sub>12</sub>CO<sub>3</sub>·4H<sub>2</sub>O had revealed that its thermal decomposition occurs from 120 to 600 °C, forming after the last step CuO and CuAl<sub>2</sub>O<sub>4</sub>, with intermediate phase of mixed oxide. The LDH/Pd1 and LDH/Pd2 presents Pd<sup>0</sup> impregnated on the surface, and the LDH/Pd3 presents [PdCl<sub>4</sub>]<sup>2-</sup> intercalated in the interlayer space. The thermogravimetric analysis was able to distinguish the mode of supporting palladium between the composites being a reliable characterization for such task.

**Acknowledgements** This research was supported by CNPq, FAPERJ and CAPES.

## References

1. Cavani F, Trifirò F, Vaccari A. Hydrotalcite-like anionic clays: preparation, properties and applications. *Catal Today*. 1991;11:173–301.
2. Vaccari A. Preparation and catalytic properties of cationic and anionic clays. *Catal Today*. 1998;41:53–71.
3. Mills SJ, Christy AG, Génin JMR, Kameda T, Colombo F. Nomenclature of the hydrotalcite supergroup: natural layered double hydroxides. *Miner Mag*. 2012;75:1289–336.
4. Miyata S. Anion-exchange properties of hydrotalcite-like compounds. *Clays Clay Miner*. 1983;31:305–11.
5. Crepaldi EL, Valim JB. Hidróxidos duplos lamelares: síntese, estrutura, propriedades e aplicações. *Quím Nova*. 1998;21:300–11.
6. Zheng L, Wu T, Kong Q, Zhang J, Liu H. Improving flame retardancy of PP/MH/RP composites through synergistic effect of organic CoAl-layered double hydroxide. *J Therm Anal Calorim*. 2017;. doi:10.1007/s10973-017-6231-6.
7. Dong Y, Zhu Y, Dai X, Zhao D, Zhou X, Qi Y, Koo JH. Ammonium alcohol polyvinyl phosphate intercalated LDHs/epoxy nanocomposites Flame retardancy and mechanical properties. *J Therm Anal Calorim*. 2015;122:135–44.
8. Silva AC, de Souza ALF, Simão RA, Malta LFB. A simple approach for the synthesis of gold nanoparticles mediated by layered double hydroxide. *J Nanomater*. 2013;2013:1–6.
9. Chen T, Zhang F, Zhu Y. Pd nanoparticles on layered double hydroxide as efficient catalysts for solvent-free oxidation of benzyl alcohol using molecular oxygen: effect of support basic properties. *Catal Lett*. 2013;143:206–18.
10. Silva AC, Senra JD, de Souza ALF, Malta LFB. A ternary catalytic system for the room temperature Suzuki-Miyaura reaction in water. *Sci World J*. 2013;2013:1–8.
11. Mora M, Sanchidrián CJ, Ruiz JR. Heterogeneous Suzuki cross-coupling reactions over palladium/hydrotalcite catalysts. *J Colloid Interface Sci*. 2006;302:568–75.
12. Zhang Q, Xu J, Yan D, Li S, Lu J, Cao X, Wang B. The in situ shape-controlled synthesis and structure-activity relationships of Pd nanocrystal catalysts supported on layered double hydroxides. *Catal Sci Technol*. 2013;3:2016–24.
13. Gong WL, Wang B, Aldred MP, Li C, Zhang G, Chen T, Wang L, Zhu M. Tetraphenylethene-decorated carbazoles: synthesis, aggregation-induced emission, photo-oxidation and electroluminescence. *J Mater Chem C*. 2014;2:7001–12.
14. Lee SB, Park SN, Kim C, Lee HW, Kim YK, Yoon SS. Synthesis and electroluminescent properties of 9,10-diphenylanthracene containing 9H-carbazole derivatives for blue organic light-emitting diodes. *Synth Met*. 2015;203:174–9.
15. Thomas AW, Ley SV. Modern synthetic methods for copper-mediated C (aryl)-O, C (aryl)-N, C (aryl)-S bond formation. *Angew Chem Int Ed*. 2003;42:500–44.
16. Senra JD, Aguiar LCS, Simas ABC. Recent progress in transition-metal-catalyzed C–N cross couplings: emerging approach towards sustainability. *Curr Org Synth*. 2011;8:53–78.
17. Sreedhar B, Arundhathi R, Reddy PL, Reddy MA, Kantam ML. Cu-Al Hydrotalcite: an efficient and reusable ligand-free catalyst for the coupling of aryl chlorides with aliphatic, aromatic and N(H)-heterocyclic amines. *Synthesis*. 2009;15:2517–22.